A New Approach to the Analytical Formulation of the Magnetic Pressure in Liquid Metal Deformation

S.M.H. Mirhoseini, Alireza Gholipour, K van Reusel, J Driesen

A New Approach to the Analytical Formulation of the Magnetic Pressure in Liquid Metal Deformation

S.M.H. Mirhoseini[1], Alireza Gholipour[2], K. Van Reusel[2] and J. Driesen[2]

[1] Applied Physics and Applied Mathematics Department, Columbia University
500 West, 120th Street, New York, 10027NY, USA
[2] Department of Electrical Engineering, KU Leuven – ESAT
Kasteelpark Arenberg 10, B-3001 Leuven, Belgium

Corresponding author: shm2148@columbia.edu

Abstract
This work deals with investigating the electromagnetic deformation of liquid metals due to magnetic pressure. First, the distribution of the magnetic fringing field produced by a gapped AC inductor in presence of a liquid metal pool is analytically investigated. The analytical method uses a combination of the direct solution of the scalar magnetic potential together with the mirror image method and conformal mapping. In the next step, the liquid metal pool deformation by the magnetic pressure produced by the gapped inductor is analytically formulated. The model is based on the Young-Laplace equation which is pressure equilibrium over the surface of the liquid metal. The surface contour of the liquid metal pool appears in the results of the differential equation. The non-dimensionalized differential equation is solved by the use of Green's functions. The proposed method is able to calculate the liquid metal pool deformation in 2D. The analytical approach is validated by the results obtained from experimental tests.
Key words: Liquid metal MHD, Meltpool deformation, Magnetic fringing field calculation

Introduction
The control of the free surface of liquid metals is of great importance for liquid metallurgical industries. During the electromagnetic processing, the free surface of the liquid metal is often prone to instability [1]. The problem of liquid metal pool deformation by means of magnetic pressure includes a capillary problem in which two different phenomena must be coupled together: *Electromagnetic and Hydrostatic problems.*

Magnetic fringing field of a gapped coil in presence of liquid metal
The scheme of the system is demonstrated in Figure 1. Assuming good electrical conductivity of the liquid metal and high enough frequency of the electric current in the coil, the magnetic fringing field of the gapped coil does not penetrate the pool. So it makes a path over the liquid sheet. To study the effect of the liquid metal pool on the magnetic fringing field, a combination of direct calculation of scalar magnetic potential, mirror image method and conformal mapping is applied. The calculation starts by using the analytical results presented by Roshen [2], where a direct calculation of the Laplace equation for the scalar magnetic potential of the gapped coil is obtained by applying the proper boundary conditions at the edge of the coil ($x = 0$). It is possible to show that the magnetic field at the fringing area ($x > 0$) in the absence of liquid metal can be calculated from (1) and (2) [2]:

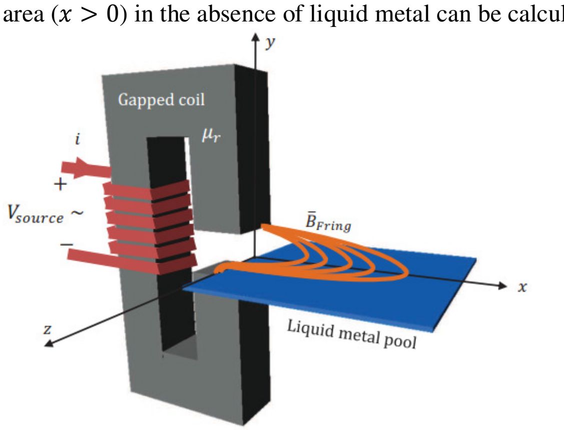

Fig. 1: Scheme of the magnetic system: Liquid metal pool is set at the edge of the gapped AC coil, causing a deformation of the magnetic field lines.

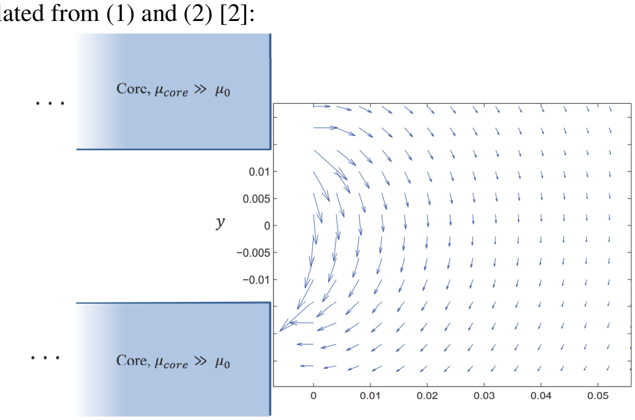

Fig. 2: Magnetic field vectors calculated by Equations (1) and (2) in the (x, y) plane

$$H_x(x,y) = -\frac{H_g}{2\pi}\ln\left(\frac{x^2+(y-l_g)^2}{x^2+(y+l_g)^2}\right) \tag{1}$$

$$H_y(x,y) = -\frac{H_g}{\pi}\left(\tan^{-1}\left[\frac{2xl_g}{x^2+y^2-l_g^2}\right]+m\pi\right) \tag{2}$$

where *m=0* if $x^2+y^2>l_g^2$ and *m=1* if $x^2+y^2\le l_g^2$. Figure 2 demonstrates the magnetic field vectors of $\overline{H}=H_x\hat{x}+H_y\hat{y}$ calculated by Equations (1) and (2) in the $x-y$ plane, where l_g is the gap length and H_g is the mean magnetic field at the airgap of the coil and is equal to $0.8NI_{coil}/2l_g$ with N number of turns, I_{coil} the current amplitude of the coil and $2l_g$ as the gap size and .

Assuming good electrical conductivity of the liquid metal and high enough frequency of the electric current in the coil, the magnetic fringing field of the gapped coil does not penetrate the pool. So it makes a path over the liquid sheet. The effect of the liquid metal is initially inserted into the problem by applying the mirror image method. This method represents a surface in the problem on which there is no perpendicular component of the magnetic field. This means that the mirror surface is a perfect conductor that does not allow the magnetic field lines to pass through. The resulting magnetic field is calculated by applying the superposition law, shifting the magnetic source shown in Fig. 1 to the distances $+d$ and $-d$ in the $x-y$ plane. The resulting magnetic field can be written as [3], [4], [5] (Fig. 3):

$$H_x(x,y) = -\frac{H_g}{2\pi}\left(\ln\left(\frac{(x+d)^2+\left(y-l_g\right)^2}{(x+d)^2+\left(y+l_g\right)^2}\right)-\ln\left(\frac{(x-d)^2+(y-l_g)^2}{(x-d)^2+(y+l_g)^2}\right)\right) \tag{3}$$

$$H_y(x,y) = -\frac{H_g}{\pi}\left(\tan^{-1}\left[\frac{2(x+d)l_g}{(x+d)^2+y^2-l_g^2}\right]+m\pi+\tan^{-1}\left[\frac{2(d-x)l_g}{(d-x)^2+y^2-l_g^2}\right]+n\pi\right) \tag{4}$$

where *d* is the distance of the mirror wall from the either magnetic sources, *m = 0* if $(x+d)^2+y^2>l_g^2$, *m = 1* if $(x+d)^2+y^2\le l_g^2$, *n = 0* if $(x-d)^2+y^2>l_g^2$ and *n = 1* if $(x-d)^2+y^2\le l_g^2$.

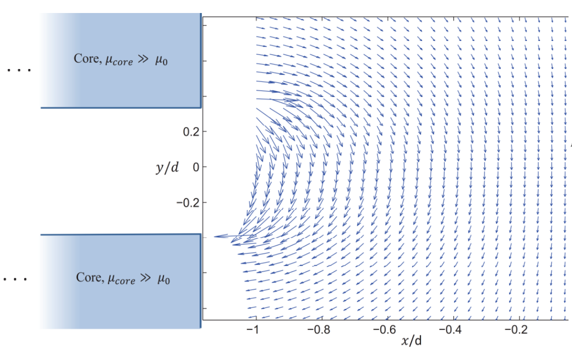

Fig. 3: Vector demonstration of the magnetic flux density in the presence of the mirror wall at *x/d=0*, calculated by (3) and (4) in the $x-y$ plane.

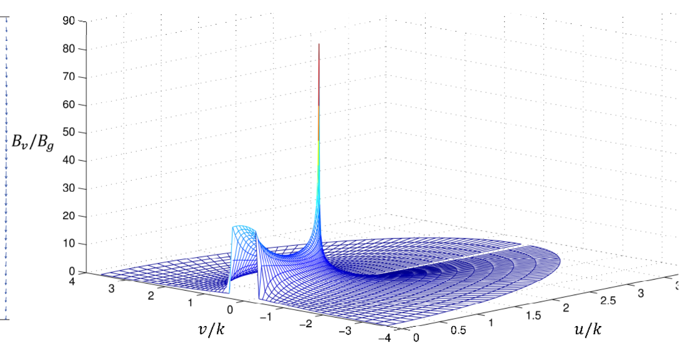

Fig. 4: Normalized magnetic flux density in the v direction for the u – v plane in the presence of liquid metal pool.

In the next step, the final feature of the problem is formed by the application of *Conformal Mapping* to the results obtained by the mirror image method, where hyperbolic cosine mapping is used. If $z = x + iy$ and $w = u + iv$, the transformation $w = k.\cosh z$ where k is a constant, will transform a series of lines parallel to the *x*-axis, and in the z-plane, to a series of confocal hyperbolas in the *w*-plane. By expanding, the expressions for *u* and *v* could be obtained:

$$u = k\cosh x\cos y \tag{5}$$

$$v = k\sinh x\sin y \tag{6}$$

The magnetic field in the u – v plane has two $\hat{u}$ and $\hat{v}$ components according to (7):

$$\overline{H}(u,v) = -\nabla\Psi(u,v) = -\frac{\partial\Psi}{\partial u}\hat{u}-\frac{\partial\Psi}{\partial v}\hat{v} \tag{7}$$

with Ψ being the scalar magnetic potential distribution in the *u*-*v* plane. One may link this relation to the magnetic field in the *x*−*y* plane using (8) and (9):

$$H_u = -\frac{\partial\Psi}{\partial u} = -\frac{\partial\Psi}{\partial x}\frac{\partial x}{\partial u}-\frac{\partial\Psi}{\partial y}\frac{\partial y}{\partial u} = H_x\frac{\partial x}{\partial u}+H_y\frac{\partial y}{\partial u} \tag{8}$$

$$H_v = -\frac{\partial\Psi}{\partial v} = -\frac{\partial\Psi}{\partial x}\frac{\partial x}{\partial v} - \frac{\partial\Psi}{\partial y}\frac{\partial y}{\partial v} = H_x\frac{\partial x}{\partial v} + H_y\frac{\partial y}{\partial v} \tag{9}$$

Finding the values for $\frac{\partial x}{\partial u}, \frac{\partial x}{\partial v}, \frac{\partial y}{\partial u}$ and $\frac{\partial y}{\partial v}$ [6], we may calculate the magnetic field distribution in the presence of the liquid metal. Figure 4 shows the normalized v component of the magnetic flux density in the u-v plane, where liquid metal pool exits at $\frac{u}{k} > 1$. The calculated magnetic field distribution will be applied to the static MHD calculations in the next section to model the liquid metal surface contour.

Analytical calculation of the melt deformation

The scheme of the system is demonstrated in Fig. 5. An AC gapped coil with $2l_g$ as the gap size, *N* the number of turns and $I_{coil}\cos(\omega t)$ the current with $\omega = 2\pi f$ and f the frequency, is used as the magnetic field source. The fringing field of the coil is applied on the surface of the liquid metal pool. The magnetic permeability of the melt μ_f is the same as that of the free space, with σ_f as the electrical conductivity, ρ as the density, and γ as the surface tension. The meltpool surface contour (*h(x)*) is a function of the distance, expressed by the horizontal coordinate (*x*). The combination of the effects regarding the downward gravitational force and the surface tension will lead to a deformation of the liquid pool surface contour, like the scheme in the Fig. 5(c). The surface tension effect on the capillary pressure difference between two immiscible fluids is given by the Young-Laplace equation [7]:

$$\Delta p = -\gamma\bar{\nabla}.\bar{n} + p_m \tag{10}$$

where Δp is the pressure difference, $\bar{n}$ is the normal vector of the surface of the metal pool. Applying the initial values and boundary conditions in [5, 6, 8] one may solve (10) using Green's function as:

$$\begin{aligned} h(x) = &\int_0^x G_R(x|\xi)\left(\frac{\sqrt{B_0}}{\sinh\sqrt{B_0} + \frac{1-\cosh\sqrt{B_0}}{\tanh\sqrt{B_0}}}(\tan\theta - \tan\theta_M) + k_M f_I(\xi)\right)d\xi \\ &+ \int_x^{L_C} G_L(x|\xi)\left(\frac{\sqrt{B_0}}{\sinh\sqrt{B_0} + \frac{1-\cosh\sqrt{B_0}}{\tanh\sqrt{B_0}}}(\tan\theta - \tan\theta_M) + k_M f_I(\xi)\right)d\xi \end{aligned} \tag{11}$$

where G_L and G_R are the left and right Green's functions that act with respect to the singularity point ξ, L_C is the length of the meltpool (Fig. 5(b)), B_0 is the Bond number, θ is the contact angle, θ_M is the correction contact angle, k_M (equal to $\mu_f H_g^2 L_{C0}/2\gamma$) is the MHD pressure constant and f_I is the horizontal distribution of the magnetic field on the surface of the liquid metal pool at (*h(x) = 0*). The resulting surface contour is demonstrated in Fig. 6. The free surface of the melt in the middle at the relaxed situation (Fig. 6(a)) is equal to the capillary length. Figure 6 shows the liquid metal pool from the relaxed situation 6(a) till the deformed situation by $k_M = 1000$. The two edges of the liquid pool at *x = 0* and *x = 1* are in contact with the horizontal surface (*h(x) = 0*). The contact angle is equal to the assumed value, $\theta = \pi/6$. It is obvious that by applying the magnetic pressure, due to the constant volume constraint, the contact point moves farther from the magnetic source and liquid metal squeezing happens. Experimental tests are shown in the Fig. 7(a)-(d), where a liquid pot (dimension is 8cm × 4cm × 1cm) containing Wood's (melting point is 70ºC, density is 9700kh/m^3, electrical conductivity is 1.39×10^6 S/m) metal is exposed to the magnetic fringing field of a gapped coil (gap length is 3cm, coil dimension is 28cm×14cm×5cm, winding turns are 20, wire diameter is 1cm), carrying a current of 0-400A, 5kHz. A comparison between the analytical and experimental results is demonstrated in Fig. 8, where the normalized maximum deformation in the *x*-direction is assumed as the melt deformation.

Conclusion

It is obvious that by applying the magnetic pressure, the deformation increases in the melt. In the current range, less than 300A, the analytical method shows an overestimation. This happens because of an overestimation of the calculated magnetic field for the lower values of the deformation. The actual radius of the liquid Wood's metal pool at the edge is around 2mm. However, considering this value for the analytical calculation of the magnetic field, will make the thickness of the modeled liquid metal pool several times higher than the real depth of the liquid metal pool in the relaxed situation (e.g. h_0). Therefore, the edge radius is considered less than the reality, which leads in a higher magnetic field at the edge and consequently a higher deformation.

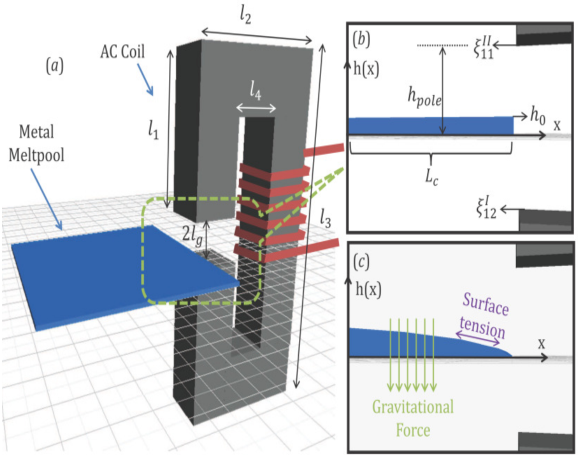

Fig. 5: Scheme of the system including gapped AC coil beside the molten metal pool (a), different parameters (b) the expected effect of surface tension and gravitational force on the melt contour (c).

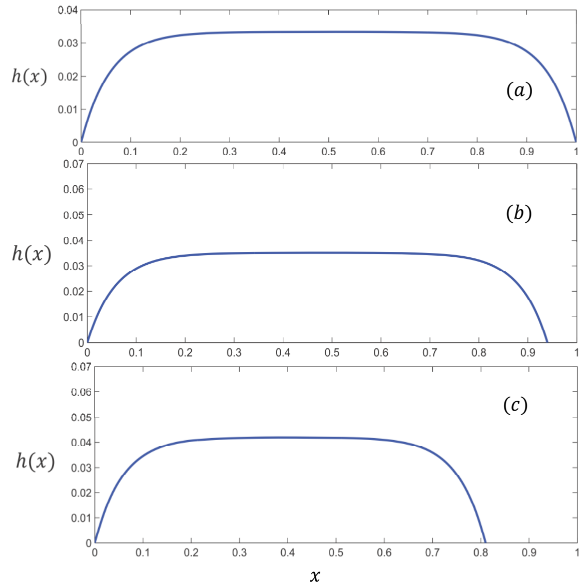

Fig. 6: Normalized magnetic flux density in the v direction for the u – v plane in the presence of liquid metal pool.

Fig. 7: Liquid metal pool deformation by means of magnetic pressure at different levels of current applied to the inductor; a) I=0A, b) I=100A c) I=200A, d) I=400A, 5kHz

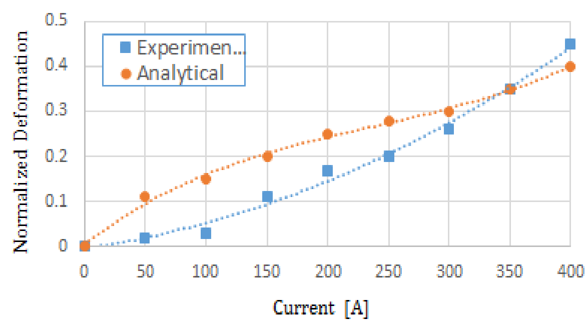

Fig. 8: Comparison between the experimental and the analytical results; the deformation $(L_c - 1)$ is normalized with the length of the liquid metal pool as a length scale. Current amplitude appears in the MHD pressure constant k_M, where it is related to the calculated deformation.

References

[1] K. J. Spragg, PhD Thesis (2009). University of Waikato.

[2] W. A. Roshen, IEEE Transactions on magnetics (2007), vol. 43, pp. 3387–3394.

[3] S.M.H. Mirhoseini, K. Van Reusel and J. Driesen, Investigation of Meltpool Deformation by Magnetic Pressure: Analytical and Experimental, MEP (2014), September 16-19, Hannover, Germany

[4] S.M.H. Mirhoseini, K. Van Reusel and J. Driesen . Analytical Approach to Meltpool Control by Magnetic Pressure, HES (2013), 21-24 May, Padua, Italy.

[5] S.M.H. Mirhoseini, K. Van Reusel and J. Driesen, Meltpool Deformation by Magnetic Pressure: Analytical and Experimental Approach, Journal of Magnetohydrodynamics, vol. 51, No. 1, 105-120, 2015.

[6] S.M.H. Mirhoseini, A. Alemany, Analytical Calculation of Thermoacoustic Magnetohydrodynamic (TA-MHD) Generator, PAMIR2014, Riga, Latvia.

[7] M. Conrath, C. Karcher, European Journal of Mechanics B/Fluids, vol. 24 (2005), pp. 149–165.

[8] S.M.H. Mirhoseini, Mathematical and Experimental Approach to Static and Dynamic MHD Problems Meltpool Control and Thermoacoustic-MHD Generator, Ph.D. Thesis, KU Leuven, 2015.